

# Journal of Photonics for Energy

[SPIDigitalLibrary.org/jpe](http://SPIDigitalLibrary.org/jpe)

## **Ridge aperture antenna array as a high efficiency coupler for photovoltaic applications**

Edward C. Kinzel  
Pornsak Srisungsitthisunti  
Xianfan Xu

# Ridge aperture antenna array as a high efficiency coupler for photovoltaic applications

Edward C. Kinzel, Pornsak Srisungsitthisunti, and Xianfan Xu

Purdue University, School of Mechanical Engineering and Birck Nanotechnology Center,  
West Lafayette, Indiana 47907-2088

[xxu@ecn.purdue.edu](mailto:xxu@ecn.purdue.edu)

**Abstract.** Weak absorption of light near the absorption band edge of a photovoltaic material is one limiting factor on the efficiency of photovoltaics. This is particularly true for silicon thin-film solar cells because of the short optical path lengths and limited options for texturing the front and back surfaces. Directing light laterally is one way to increase the optical path length and absorption. We investigate the use of a periodic array of apertures originated from bowtie aperture antennas to couple incident light into guided modes supported within a thin silicon film. We show the presence of the aperture array can increase the efficiency of a solar cell by as much as 39%. © 2011 Society of Photo-Optical Instrumentation Engineers (SPIE). [DOI: [10.1117/1.3644613](https://doi.org/10.1117/1.3644613)]

**Keywords:** aperture array; ridge waveguide; photovoltaic.

Paper 11186PR received Mar. 23, 2011; revised manuscript received Aug. 3, 2011; accepted for publication Sep. 9, 2011; published online Sep. 29, 2011.

## 1 Introduction

Thin-film solar cells have the potential to dramatically improve the economics of photovoltaics. The thickness of active region in a thin-film cell is generally  $<2 \mu\text{m}$ .<sup>1,2</sup> This allows the semiconductor deposited on and supported by inexpensive substrates such as glass, which further reduces the manufacturing and handling costs. The low-cost, long-term availability, low-toxicity, and mature processing technology continue to make silicon a good choice for photovoltaic applications.<sup>1</sup> However, the optical absorptivity of crystalline and polycrystalline silicon, particularly near the band edge, is poor. For example, the absorption depth for crystalline silicon is  $<100 \text{ nm}$  for  $\lambda_0 < 407 \text{ nm}$ ; however, it is  $\sim 10 \mu\text{m}$  for  $\lambda_0 > 710 \text{ nm}$  and approaches hundreds of micrometers near the band edge. This necessitates the use of relatively thick pieces (200 to 300  $\mu\text{m}$ ) of silicon to effectively capture the solar spectrum. In addition to the optical requirements for the semiconductor, the minority carrier diffusion length must be several times the semiconductor thickness in order for all carriers to be collected.<sup>1,3</sup> This has led to the widespread use of wafer-based crystalline silicon solar cells<sup>1,2</sup> where the wafers contribute a substantial portion of the expense of the module.<sup>2</sup> The electrical and manufacturing cost benefits in thin-film silicon solar cells come at the expense of the optical performance. In wafer-based crystalline solar cells, pyramidal structures are typically employed to increase the optical path length. These structures are 2 to 10  $\mu\text{m}$  thick and thus are not suitable for thin-film solar cells.<sup>1,2</sup>

Recently, plasmonics have been proposed as one way of trapping light in thin semiconductor films.<sup>1-5</sup> These designs incorporate metal features to couple incident light into the thin film. They generally combine confining light in the immediate vicinity of the metallic structure, exciting local surface plasmons (LSP) and/or scattering light into propagating modes within the semiconductor film to increase the optical path length. The propagating modes can be either based on long-range surface plasmon polaritons (SPP), which are trapped along the semiconductor/metal surface or confined in a semiconductor. Several different plasmonic light-trapping approaches have been proposed. These include placing metallic nanoparticles on the

front surface of the cell<sup>2,4</sup> or embedding them within the semiconductor.<sup>1</sup> Similarly, patterned grating-like features can be incorporated into the cell, either on the front surface<sup>6</sup> or etched into the back conductor.<sup>1,3,5</sup>

In this work, we study an aperture array on the front surface of the semiconductor. Similar to the front surface gratings, the apertures trap the light in the semiconductor via scattering in addition to LSP resonances. We focus on a 225-nm thick polycrystalline silicon film, with the goal of achieving broadband, polarization-insensitive absorption enhancement. The antenna array is designed using bowtie apertures as basic elements. In isolation, these apertures have been shown to be able to couple light into propagation mode parallel to the surface with high efficiency.<sup>7</sup> In this letter we optimize an array of these apertures to maximize the fraction of the light absorbed by a thin silicon film. This involves lowering the reflection, as well as losses, due to absorption in the metal.

## 2 Numerical Analysis

Figure 1 shows the geometry of our system. It consists of a glass superstrate, metal apertures, a silicon film, and an optically thick metal layer. We select this configuration so that the metal apertures can be patterned using e-beam lithography or nanoimprint lithography which is facilitated by limiting the pattern thickness to 25 nm. An advantage of the front-contact configuration is that the aperture array can serve as the front contact for the solar cell. Silver is selected for the metal apertures and the top metal layer because of its low losses at optical frequencies. This silver layer is encapsulated between the fused silica and silicon; therefore oxidation will not be a concern, although in an actual device a barrier oxide is required to prevent migration of silver into the semiconductor. The total thickness of the silicon layer is  $h = 225$  nm. Optical properties of silicon and silver are taken from Refs. 8 and 9, respectively, and that of glass is taken as  $n = 1.46$  across the spectrum of interest.

The geometry of the aperture array is defined by the outline dimension  $a$ , periodicity  $p$ , gap dimension  $g$ , and the two angles  $\alpha$  and  $\beta$ , as shown in Fig. 1(a). Radii of curvature  $r_1$ ,  $r_3$ , and  $r_4$  are selected to be 25, 25, and 10 nm, respectively, to represent practical fabrication. We optimize the structure in Fig. 1 using the frequency domain finite element method.<sup>10</sup> The results indicate the optimized absorption are obtained for  $\alpha = 75$  deg and  $\beta = 110$  deg. The periodicity of the array is based on the outline dimension,  $p = a + 150$  nm. The thickness of the metal portions of the structure (the separation between adjacent apertures) is fixed at 50 nm. The gap  $g$  is fixed at 25 nm, which is limited by typical nanofabrication methods. A plane wave is normally incident from the glass side.

To maximize the open area of the array and remove the polarization sensitivity, we tessellate bowtie apertures. The bowtie aperture is one geometry of ridge waveguide which has been studied at optical frequencies.<sup>11</sup> When isolated (not in an array), bowtie apertures confine the electric field to the gap region, defined by  $g$ , which can be much smaller than the wavelength of light. This feature has been previously applied to nanolithography<sup>12</sup> and nanometer scale sensing.<sup>13</sup> An additional feature of bowtie apertures is that they produce a magnetic dipole

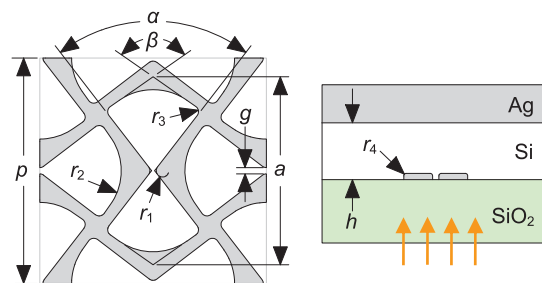


**Fig. 1** Schematic of solar cell geometry.

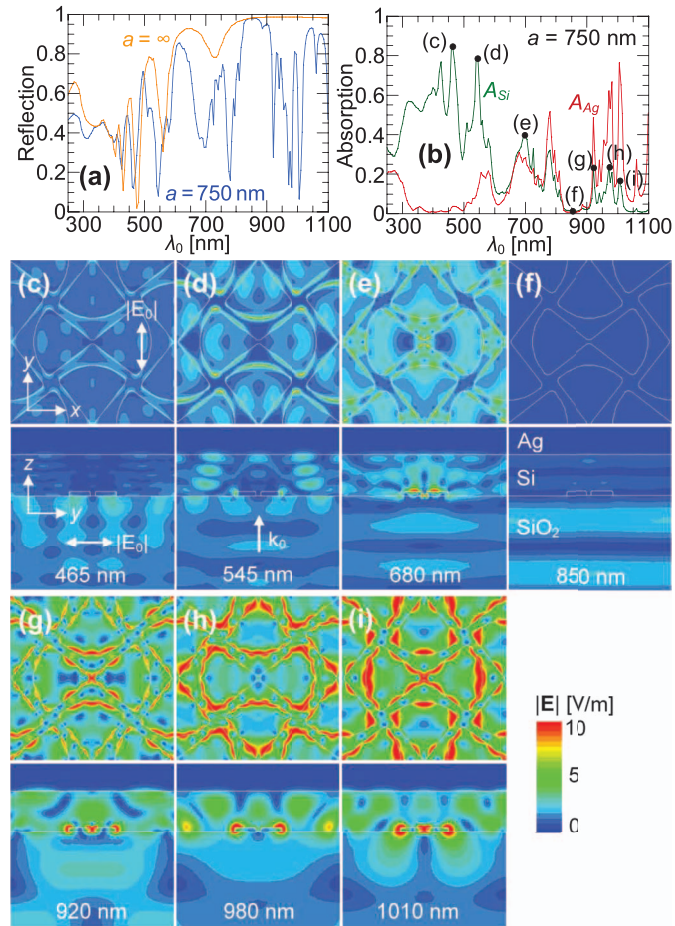


**Fig. 2** Results for an aperture array defined by  $a = 750$  nm. (a) Reflection from aperture array in comparison to a bare silicon film. (b) Absorption in the silicon layer and losses in the silver films. (c)–(i) Electric field distributions at a number of wavelengths. Top row: electric field mid-way through the apertures; bottom row, cross-section view. The electric field intensity of the exciting plane wave is 1 V/m and the plots are saturated at 10 V/m.

which couples efficiently to and from SPP and guided modes along the film that the aperture is defined in Refs. 7 and 14. In these previous studies, bowtie apertures show large polarization sensitivity, i.e., light coupling is orders of magnitude higher in one direction (the direction across the gap) than the other. By orienting the bowtie apertures in both directions as shown in Fig. 1, the polarization sensitivity is minimized for photovoltaic applications.

We determine the power dissipated in silicon and silver layers as well as the light that is reflected from the system over the wavelength range  $\lambda_0 = 250$  to 1110 nm in 5 nm increments. Since the materials have a negligible magnetic response at optical frequencies, the absorption at any point is given by:  $P = 0.5\sigma|E|^2$ , where  $\sigma$  is the conductivity of either silicon or silver (no power is dissipated in the glass). We determine the fraction of power absorbed by normalizing  $P$  (integrated over the volume) to the power in the normally incident plane wave.

Figure 2(a) shows the reflectance  $R (= 1 - A_{Ag} - A_{Si})$ , where  $A$  is absorption) for the aperture array with  $a = 750$  nm, along with  $a = \infty$  (a 225-nm thick silicon slab with no aperture array, but with a silver back layer). The figure shows that in the near-IR the aperture array reflects considerably less light than the bare silicon film. Figure 2(b) shows how much light is absorbed in the silicon and silver layers, respectively. Evidently there is enhanced absorption in silicon in the near-IR region, where the antenna array is designed for, whereas absorption in silicon

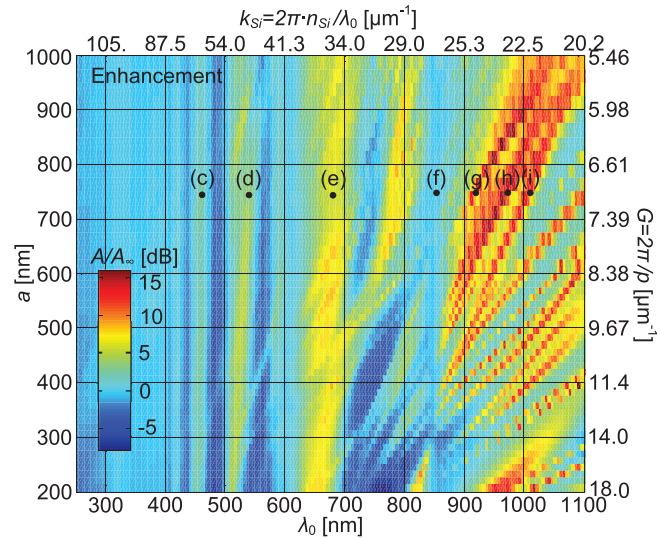


**Fig. 3** Absorption enhancement in silicon compared with that without the aperture array.

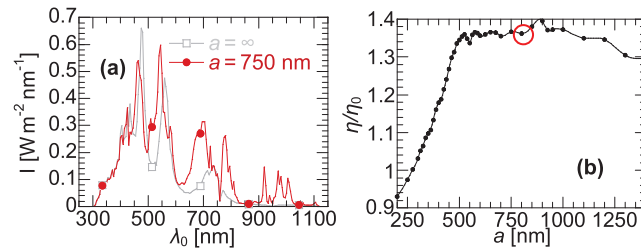
in near-IR is near zero if no antenna array is used. There are multiple spectral features in Figs. 2(a) and 2(b), which are caused by different resonance phenomena. Figures 2(c)–2(i) show the electric field through the aperture array and in cross section at wavelengths corresponding to peaks in Fig. 2(b). At short wavelengths, 465 and 545 nm, the aperture array does not significantly affect the field and the peaks are from Fabry P erot (FP) resonance. Additional enhancement near the metal corners is due to LSP. The minimum absorption in Figs. 2(b) and 2(f) is caused by FP antiresonance. The peaks at 920, 980, and 1010 nm are caused by modes in the silicon film that are being scattered off the edges of the apertures, forming standing waves as shown in Figs. 2(g) and 2(h). Collectively, light being absorbed at the wavelengths near these absorption peaks provides an enhancement compared to a bare silicon film.

Figure 3 shows a comparison between the absorption in silicon with aperture arrays normalized to the bare 225-nm thick silicon film at wavelengths up to 1100 nm, and for different aperture size  $a$ . There is little effect at short wavelengths,  $<400$  nm. From 400 to 700 nm, we see enhancements due to FP modes in the film which have little dependence on the aperture size. These modes are slightly shifted from their locations in the bare silicon slab due to the presence of the aperture array. For wavelengths longer than 700 nm, we see large enhancements dependent on the aperture size. These modes involve the aperture array trapping light in guided modes in the silicon film, the interference of which are observed as the standing waves in Figs. 2(g) and 2(h).

### 3 Results and Discussion

We consider the power the silicon film captures by assuming that each photon absorbed in the silicon generates a single carrier pair which has the energy of the band gap (1.11 eV). Figure 4(a) shows the results of this calculation for  $a = 750$  nm as well as the bare silicon film. In this case we have assumed the AM1.5 solar spectra. Although there is a slight reduction in power generation at a peak below 500 nm, the photons in the near-IR are much more efficiently absorbed.

We integrate over the solar spectra to determine the total power (per unit area) absorbed, normalized to the total intensity of the AM1.5 spectra to determine the efficiency. The maximum efficiency of our design occurs for an aperture size  $a = 900$  nm, where 12.1% of the incident light is absorbed by the silicon film. Figure 4(b) shows a comparison to the bare 225-nm thick silicon film which absorbs 8.65% of the light. Therefore, the total enhancement is 39%. Note this



**Fig. 4** (a) Power per unit area captured by the silicon film with ( $a = 750 \text{ nm}$ ) and without ( $a = \infty$ ) aperture array under illumination with AM1.5 spectra relaxed to 1.11 eV bandgap. (b) Total enhancement in efficiency for different sized apertures compared to a bare silicon film.

enhancement is thickness dependent, and is higher in thinner films. Figure 4 shows that smaller apertures, where a greater portion of the surface is blocked by silver, have a lower efficiency. The efficiency is nearly constant from  $a = 500$  to  $1000 \text{ nm}$ , above which point it starts to diminish as the aperture array approaches the limiting case of the apertureless film. The invariance with the aperture size is due in part to the convolution of the solar spectra with the absorption curve in the structure which leads to a relatively constant efficiency in the near-IR. The aperture array causes light which would not be absorbed by a bare silicon film to match coupled modes at a wavelength determined by the aperture size. Figure 3 shows that the geometry of the aperture array scatters light into multiple modes. For comparison we also simulated a simpler fishnet structure (square apertures or two-dimensional gratings formed by thin metal wires) with the same open area and periodicity ( $a = 700$ ) as the bowtie aperture array. The overall absorption in silicon is 8% better than a bare 225-nm thick film (9.5% of the light is absorbed). This shows that the bowtie aperture geometry significantly contributes to the enhancement.

## 4 Conclusion

In conclusion, we demonstrated a tessellated bowtie aperture array for enhancing absorption in silicon thin film photovoltaic solar cells. The aperture array presented in this work is polarization insensitive, and is designed as broadband as possible. It scatters light at near-IR wavelengths to guided modes trapped in the silicon film. The results showed that the aperture array can enhance solar energy coupling into a thin silicon film by up to 39%.

## Acknowledgments

Support for this work by the National Science Foundation (NSF), the Defense Advanced Research Project Agency (DARPA), and Air Force Office of Scientific Research (AFOSR)-Multidisciplinary University Research Initiative (MURI) is gratefully acknowledged.

## References

1. H. A. Atwater and A. Polman, "Plasmonics for improved photovoltaic devices," *Nature Mater.* **9**, 205–213 (2010).
2. K. R. Catchpole and A. Poleman, "Plasmonic solar cells," *Opt. Express* **16**, 21793–21800 (2008).
3. V. E. Ferry, L. A. Sweatlock, D. Pacifici, and H. A. Atwater, "Plasmonic nanostructure design for efficient light coupling into solar cells," *Nano Lett.* **8**, 4391–4397 (2008).
4. S. Pillai, K. R. Catchpole, T. Trupke, and M. A. Green, "Surface plasmon enhanced silicon solar cells," *J. Appl. Phys.* **101**, 093105 (2007).
5. W. Wang, S. Wu, K. Reinhardt, Y. Lu, and S. Chen, "Broadband light absorption enhancement in thin-film silicon solar cells," *Nano Lett.* **10**, 2012–2018 (2010).

6. R. A. Pala, J. White, E. Barnard, J. Liu, and M. L. Brongersma, "Design of plasmonic thin-film solar cells with broadband absorption enhancements," *Adv. Mater.* **21**, 3504–3509 (2009).
7. E. C. Kinzel and X. Xu, "High efficiency excitation of plasmonic waveguides with vertically integrated resonant bowtie apertures," *Opt. Express* **17**, 8036–8045 (2009).
8. E. D. Palik, *Handbook of Optical Constants of Solids*, Academic Press, San Diego (1997).
9. P. B. Johnson and R. W. Christy, "Optical constants of the noble metals," *Phys. Rev. B* **6**, 4370–4379 (1972).
10. HFSS, Ansoft LLC, <http://www.ansoft.com/products/hf/hfss/>.
11. E. X. Jin and X. Xu, "Finite-difference time-domain studies on optical transmission through planar nano-apertures in a metal film," *Jpn. J. Appl. Phys.* **43**, 407–417 (2004).
12. L. Wang, S. M. Uppuluri, E. X. Jin, and X. Xu, "Nanolithography using high transmission nanoscale bowtie apertures," *Nano Lett.* **6**, 361–364 (2006).
13. L. Wang and X. Xu, "High transmission nanoscale bowtie-shaped aperture probe for near-field optical imaging," *Appl. Phys. Lett.* **90**, 261105 (2007).
14. E. C. Kinzel and X. Xu, "Extraordinary infrared transmission through a periodic bowtie aperture array," *Opt. Lett.* **35**, 992–994 (2010).

Biographies and photographs of the authors not available.